https://doi.org/10.5194/egusphere-2026-266
Preprint. Discussion started: 23 January 2026

Seasonal Contrast in Rare Earth Elements Concentration in Sediment of the Mackenzie Delta

Thomas Bossé-Demers[1], Bennet Juhls[2], Martine Lizotte[3], Santiago Mareque[1], Audrey Gaudy[1], Raoul-Marie Couture[1,*]

[1] Département de chimie, Centre d'études nordiques, and Takuvik International Laboratory CNRS/ULaval, Université Laval, 1045 Ave. de la médecine, Québec, QC G1V 0A6, Canada
[2] Permafrost Research Section, Alfred Wegener Institute Helmholtz Centre for Polar and Marine Research, Potsdam, Germany
[3] Maurice Lamontagne Institute, Fisheries and Oceans Canada, 850 Rte de la Mer, Mont-Joli, QC G5H 3Z4, Canada

Correspondence to: Raoul-Marie Couture (raoul.couture@chm.ulaval.ca)

Abstract. This study reports on the concentration of rare earth elements (REE) along with ancillary geochemical parameters at 12 locations across the Mackenzie River, its delta and coastal waters, both under ice and in open water. Specifically, we analyzed REE, carbon, and redox-sensitive elements (Fe, Mn) in 108 sediment samples and 96 porewater and overlying water samples collected under ice before the spring freshet (April–May) and in open water in early fall (August–September). While sediment REE concentrations remained relatively stable across seasons, results revealed a striking contrast between the two sampling seasons in the porewater, where REE concentrations were nearly two orders of magnitude lower under ice (avg. 216 nmol L^{-1}) than under open water in the fall (avg. 3.20 nmol L^{-1}). Similarly, dissolved organic carbon (DOC) concentrations were approximately one order of magnitude lower under ice than in the fall. Sediment REE concentrations were positively correlated to those of Fe and Mn, particularly under ice, consistent with control by adsorption processes onto their (oxy)hydroxides. In the porewater, winter and fall samples form distinct clusters based on concentration magnitudes. Chromophoric properties of dissolved organic matter (DOM) in the overlying water suggest that under-ice DOM was characterized by low aromaticity, older material compared to the more aromatic, humic-rich DOM measured in open-water. We conclude that under-ice conditions, chiefly cold temperature, allow for DOM accumulation in the porewater, which, combined with other possible REE enrichment mechanisms in the porewater, such as REE–carbonate complex formation and exclusion during ice formation, contributes to the elevated winter REE concentrations observed here. To our knowledge, this is the first report of such large seasonal fluctuation in dissolved REE in the fluvial-marine transition zone of the Mackenzie, the largest riverine influence on the Arctic Ocean.

https://doi.org/10.5194/egusphere-2026-266
Preprint. Discussion started: 23 January 2026

1. Introduction

Arctic coastal environments and deltas represent critical biogeochemical hotspots at the interface between terrestrial and marine systems. They serve as important conduits and processing sites for trace elements and contaminants. The Mackenzie River system, which drains a large portion of northwestern Canada and discharges into the Beaufort Sea, has received particular attention for its role in transporting contaminants, with recent studies revealing pronounced seasonal and spatial patterns in mercury exposure throughout the Mackenzie watershed, linked to hydrological conditions and biogeochemical processes (Jermilova et al., 2025). These findings highlight the importance of understanding trace element cycling in Arctic river systems, where seasonal variations in temperature, organic matter dynamics, and ice cover can influence contaminant behavior.

Seasonal ice cover responds strongly to global environmental changes (Gudasz et al., 2010; Landy et al., 2022). Seasonality significantly influences elemental distribution and geochemical processes by affecting water and sediment temperatures, site salinity through ice exclusion or freshwater dilution (Degrandpre et al., 2021; Finlay et al., 2006), photosynthesis activity (Retamal et al., 2008; Semkin et al., 2022), river discharge patterns (Gareis and Lesack, 2017), and carbon input from surrounding terrestrial environments (Holmes et al., 2012; Gareis and Lesack, 2017; Liu et al., 2022). These seasonal dynamics collectively regulate environmental processes and the associated mobility and distribution of reactive elements.

Among the elements of growing scientific interest, rare earth elements (REE) offer insights both into biogeochemical processes due to their coherent geochemical behavior and sensitivity to environmental conditions (Škerlep et al., 2025; Ye et al., 2019), and as tracers of sediment sources due to their distribution representing geological signatures (Bossé-Demers et al., 2025). Interest in REE thus continues to grow due to their applications in advanced technologies and their increasing utility as proxies for environmental processes (Alonso et al., 2012; Haque et al., 2014; Tostevin et al., 2016; Guo et al., 2024; Grenier et al., 2022).

Generally, REEs tend to behave coherently in the environment due to their similar reactivity patterns and predominant oxidation state, +III (Wall, 2021; Rollinson and Pease, 2021). Organic carbon quantity and quality (i.e., aromaticity, molecular weight and functional group composition) may influence the distribution of REE through organic matter complexation, as dissolved organic compounds can form stable complexes with REE, affecting their mobility and fractionation patterns (Davranche et al., 2004; Pourret et al., 2007a, c; Marsac et al., 2021). Marginson et al. (2024) found positive dissolved organic carbon (DOC)–REE and humic-like dissolved organic matter (DOM)–REE correlations in the sub-Arctic George River, highlighting the influence of organic matter quantity and quality on REE distribution in these systems.

While dissolved REE in Arctic lakes and rivers display very different concentrations between sites with otherwise similar geochemical characteristics (Macmillan et al., 2017; Pokrovsky et al., 2016), the seasonal dynamics of sedimentary REE in cold regions remains understudied. To our knowledge, REE have never been studied in Arctic river porewater. Despite being the geochemical compartment that mechanistically connects sediment and overlying water, porewater remains comparatively understudied due to analytical challenges associated with low concentrations and limited sample (Abbott et al., 2015). Yet,

https://doi.org/10.5194/egusphere-2026-266
Preprint. Discussion started: 23 January 2026

REE cycling in sediment porewater contributes significantly their mobility in marine sediment (Abbott et al., 2015; Deng et al., 2022).

Here, we set out to better understand the magnitude and controlling factors of seasonal variations in REE concentrations. Previous work at other Arctic sites has hinted at various causes for such variation at other sites, including reduced bacterial degradation of organic matter at low temperatures preserving DOC–REE complexes (Arnosti et al., 1998), and enhanced REE–carbonate complex stability at low temperatures (Marginson et al., 2024). Here, we investigate the linkages between REE concentrations, DOC concentrations and DOM quality. To do so, we analysed REE, DOC/DOM, and Fe and Mn in sediment, overlying water and porewater samples across 12 sites during two sampling seasons in the Mackenzie River Delta. We use this unique data set to improve our understanding of seasonality effects on REE in a cold region and to better understand how these impact REE distribution.

2. Materials and Methods

2.1. Study Region

The Mackenzie River (Northwest Territories, Canada) flows into the Beaufort Sea through the second-largest delta in the Arctic. The Mackenzie drainage basin encompasses 1.8×10^6 km^2 within Canada, including the Rocky Mountains and Mackenzie Mountains. About half of this area is situated in continuous or discontinuous permafrost zones (Abdul Aziz and Burn, 2006; Hill et al., 2001; Holmes et al., 2012). The river is covered by ice from late October to late May (Hill et al., 2001). The delta exhibits pronounced seasonal and interannual discharge variability that significantly influences the Beaufort Sea (Hill et al., 2001; Mulligan and Perrie, 2019; Nghiem et al., 2014; Emmerton et al., 2008a). During winter, the river discharge diminishes under extensive ice coverage (Goñi et al., 2000; Hill et al., 2001). The ice break-up period in late May and early June triggers the spring freshet, during which snow and ice meltwater cause increased water discharge (e.g., Hill et al., 2001). By early June, freshwater extends more than 100 km from the river mouth onto the shelf (Juhls et al., 2022). Approximately 70% of annual freshwater discharge occurs between May and September (Leitch et al., 2007; Macdonald et al., 2012), with recent years showing an overall increase in discharge volume (Kopec et al., 2024; Rood et al., 2017). With the contrasting seasonal patterns, the Mackenzie River sets an ideal study site for evaluating seasonality effects on REE distribution in coastal settings.

The Mackenzie River is the principal sediment source to the Arctic Ocean. It delivers an estimated 1.28×10^{11} kg of sediment annually (Holmes et al., 2002; Stein et al., 2004) and contributes 90–95% of total sediments to the Beaufort Shelf (Vonk et al., 2015). Its sediment sources include the Peel (21×10^9 kg), Arctic Red (7×10^9 kg), and Liard ($35–45 \times 10^9$ kg) rivers (Vonk et al., 2015). The sediments are mostly composed of fine-grained silt and clay (Hill et al., 2001; Holmes et al., 2012). These sediments are transported through relatively shallow river channels reaching a maximum depth of approximately 10 m (Hill et al., 2001; Mulligan and Perrie, 2019).

https://doi.org/10.5194/egusphere-2026-266
Preprint. Discussion started: 23 January 2026

2.2. Sample retrieval and preservation

The Mackenzie River and its downstream coastal areas were sampled within the context of the EU-H2020 project Nunataryuk. Research teams collected various physicochemical parameters at these sites, with their data and conclusions available in separate publications (Juhls et al., 2022; Bertin et al., 2023; Lizotte et al., 2023). Sampling was performed across two rivers to coast transects along the western and eastern outflow area of the Mackenzie River during two distinct periods: before the spring freshet in April and May 2019, with fully ice-covered sites (labeled W in Table 1), and in early fall in August and September 2019, representative of open-water conditions at the end of the season of high biological productivity (labeled F in Table 1). This corresponds to Leg 1 (17 April to 3 May 2019) and Leg 4 (26 August to 9 September 2019) of the Nunataryuk field campaigns (Lizotte et al., 2023). These sampling campaigns took place before and after large freshwater and sediment discharge events occurring during the summer. Hereafter, we name those sampling periods "winter" and "fall" as they represent those respective conditions. The western sampling transects extended from Inuvik (68.35°N, 133.68°W) towards the western river mouth and the coastal waters of the Mackenzie Bay (69.14°N, 136.85°W). The eastern transects ran from the east river mouth to the coastal water of Kugmallit Bay (69.66°N, 133.23°W), as presented in **Fig. 1**.

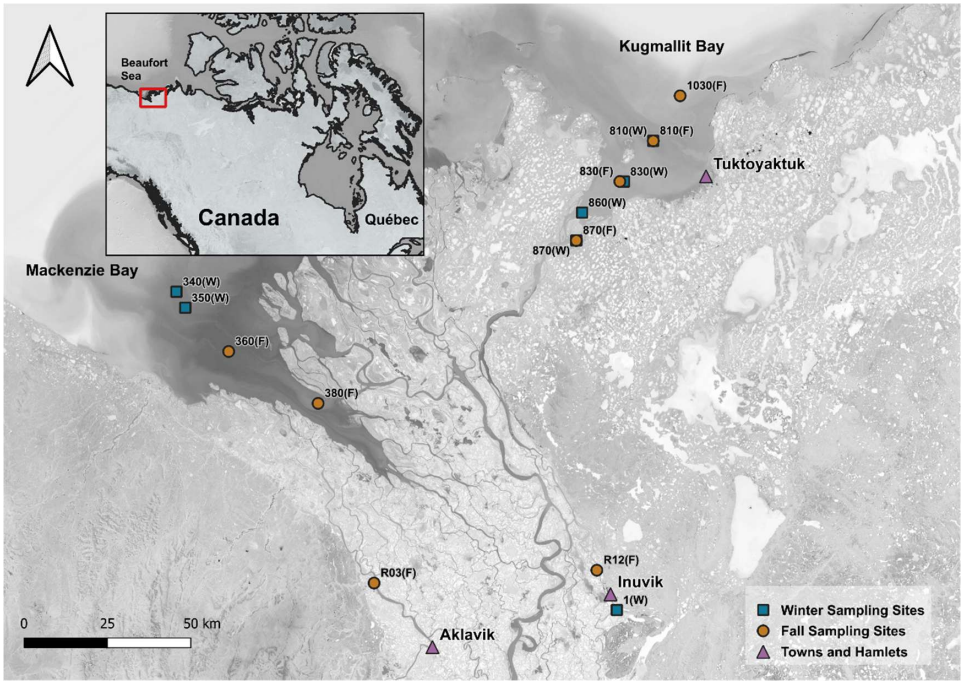

Figure 1: Sampling sites across the Mackenzie Delta. Squares (blue) represent winter sampling sites and circles (brown) represent fall sampling sites. Towns and hamlets are shown by triangles (purple). (Source: ESRI | Powered by Esri)

https://doi.org/10.5194/egusphere-2026-266
Preprint. Discussion started: 23 January 2026

Table 1: Sampling station channel, water column depth, geographical coordinates, and bottom water temperature.

*Site**	*Channel*	*Water Depth (m)*	*Lat. (N)*	*Lon. (W)*	*Temp. (°C)*
340(W)	*West*	*3.1*	*69.151*	*136.855*	*0.0*
350(W)	*West*	*2.2*	*69.110*	*136.791*	*0.0*
1(W)	*River*	*1.5*	*68.319*	*133.678*	*0.1*
860(W)	*East*	*4.2*	*69.353*	*133.928*	*0.0*
810(W)	*East*	*1.8*	*69.535*	*133.415*	*0.0*
870(W)	*East*	*4.8*	*69.289*	*133.969*	*0.0*
830(W)	*East*	*1.5*	*69.432*	*133.626*	*0.0*
360(F)	*West*	*0.9*	*68.997*	*136.478*	*7.3*
380(F)	*West*	*1.3*	*68.863*	*135.833*	*10.2*
R03(F)	*River*	*3.5*	*68.391*	*135.429*	*9.4*
R12(F)	*River*	*3.2*	*68.425*	*133.822*	*10.2*
810(F)	*East*	*1.8*	*69.535*	*133.415*	*8.2*
870(F)	*East*	*4.8*	*69.282*	*133.970*	*10.6*
830(F)	*East*	*0.3*	*69.432*	*133.656*	*10.1*
1030(F)	*East*	*4.3*	*69.648*	*133.221*	*5.6*
340(F)	*West*	*2.4*	*69.152*	*136.857*	*7.5*
840(F)	*East*	*0.6*	*69.399*	*133.809*	*10.4*

** (W) Sampled in late winter. (F) Sampled in early fall.*

Sediment was sampled with a gravity corer (UWITEC, Austria) with a 9-cm diameter core liner. Winter, under ice sampling was conducted through a hole in the ice, with the gravity corer maintained using a tripod. Sites were accessed via helicopter or snowmobile. Fall sampling was conducted on a boat. At each site, duplicate sediment cores were taken, with one used for sediment subsampling at 1-cm intervals and the other for porewater extraction (see below). Subsampling was conducted at the Aurora Research Institute (ARI) in Inuvik for western sites and at the Tuktoyaktuk Learning Center for eastern sites. Subsamples were placed in Falcon cups (Corning, USA) and frozen. Back in the laboratory at Université Laval, frozen sediment samples were freeze-dried and homogenized using an agate mortar and pestle. Aliquots of these homogenized samples were used for subsequent solid phase analyses.

Porewater was sampled from pre-drilled core liners with holes covered by tape at 1-cm intervals. Upon retrieving the core, acid-washed 5-cm Rhizon samplers (Rhizosphere Research, Netherlands) with 0.15-µm PES membranes were inserted into the core. Porewater was retrieved using acid-washed syringes (VWR, Canada) by creating a vacuum. This allowed collection of 7–10 mL of porewater (Seeberg-Elverfeldt et al., 2005), starting at 1 cm above the sediment-water interface (the overlying water) and continuing down to the depth where bottom clays prevented Rhizons insertion (5–20 cm). The collected porewater was distributed into different vials for preservation. For DOC concentration and DOM quality measurements, 2 mL of porewater were delivered to amber glass vials fitted with Teflon-lined caps. The vials were previously cleaned in hydrochloric acid (HCl) (10%) baths followed by sodium hydroxide (NaOH) (0.1 M) baths and ultrapure water baths for 24 hours each, then combusted at 450°C overnight. Teflon-lined caps were washed separately in an ultrapure water bath. For major and trace

https://doi.org/10.5194/egusphere-2026-266
Preprint. Discussion started: 23 January 2026

elements, samples were transferred to 15-mL clear vacuette tubes polyethylene terephthalate (PET) for the winter samples or 15-mL high-density polyethylene (HDPE) centrifuge tubes for the fall samples. Both containers were acid washed in 4% nitric acid (HNO_3) baths and rinsed with ultrapure water baths prior to use. Approximately 4 mL of porewater sample was amended with 320 µL of 50% double-distilled Omnitrace HNO_3 (Fisher Scientific, Canada) to obtain a final concentration of ≈ 4% HNO_3 suitable for preservation.

Prior to major and trace metal analysis in the sediment, 50 mg of homogenized sediment was placed in a Teflon microwave reaction vessel (EasyPrep, CEM Corporation, Canada) amended with 6.5 mL of Aristar Plus 12 M HCl (VWR Canada) and 3.5 mL of doubled-distilled 16 M Omnitrace HNO_3 (Fisher Scientific, Canada). A procedural blank and a certified reference material sample (CRM MESS-4, NRC Canada) were included in the microwave carousel. The samples were digested in a MARS 5 microwave (CEM Corporation, Canada) with a 20-minutes ramp to 1,600 W (setting of maximum 800 PSI 240°C), followed by a 20-minute hold time and a 30-minute cooling period. After digestion, the samples remained in the vessels overnight to cool completely. The vessels were opened and placed on a temperature-controlled Digiprep block (SCP Sciences, Canada) for evaporation at 120°C for approximately 3.5 hours, until nearly dry. The samples were then transferred under a laminar flow hood (ESCO, USA) for recovery in 2.87 mL of doubled-distilled 16 M Omnitrace HNO_3 (Fisher Scientific, Canada). This solution was then transferred to an acid-washed 50-mL HDPE centrifuge tube (VWR Canada). The Teflon vessels were rinsed three times with ultrapure water, and the solution was added to the centrifuge tube. The final solution was brought to a volume of 50 mL to achieve ≈4% HNO_3.

2.3. Instrumental Analysis

Major elements in the sediments were analyzed by ICP-OES (Thermo Scientific iCAP 7400, USA) using Iridium (Ir) as an internal standard. Analysis of the digested CRM MESS-4 yielded accuracy greater than 98% for Fe (n = 11) and 91% for Mn (n = 9). REE in the sediment were measured by triple-quadrupole ICP-MS (Agilent 8900, Agilent Canada) using Iridium (Ir) as an internal standard. The method for REE in sediment was validated using MESS-4 reference material, yielding accuracy greater than 91% for La, Ce and Eu (n = 21), and greater than 75% for Nd (n = 12). Lu could not be assessed due to low recovery rates. REE in the porewater were also analyzed by ICP-QQQ-MS, using Te and Rh as internal standard. The method for REE in porewater was validated using the CRMs SLRS-6 (NRC Canada) and TM-DWS.3 (Environment and Climate Change, Canada), with accuracy exceeding 92% (n = 3) for all analytes. The analyses were performed in O_2-mode with a collision cell to minimize isobaric interferences for REE and Fe, while Mn was performed in single-quad mode. For concentration values under the detection limit, half detection limit was used to enable statistical analysis.

Solid-phase carbon content in the sediment was determined using a CHN analyzer (Flash 2000, Thermo Scientific, Canada). Homogenized sediment samples (3 mg) were weighed and placed in tin capsules for analysis. The method was validated using reference materials (cystine and sulfanilamide), yielding accuracy greater than >99.3% (n = 10). Porewater DOC analysis was performed using a total organic carbon and nitrogen (TOC/TN) analyzer (Vario Cube, Elementar, Germany). In-house carbon standards were used to validate the method, achieving accuracy of > 90% (n = 17).

https://doi.org/10.5194/egusphere-2026-266
Preprint. Discussion started: 23 January 2026

Fluorescent DOM (FDOM) from Matsuoka et al. (2021b) were measured using a spectrofluorometer (Aqualog, Horiba, Japan) with corrections for inner-filter effects and Raman-Rayleigh scattering. Fluorescent components were identified via a parallel factor analysis (PARAFAC) modeling and compared with the OpenFluor database. Chromophoric DOM (CDOM) absorption spectra (200-722 nm) from Matsuoka et al. (2021a) were measured in triplicate within 12 hours of collection using an UltraPath liquid waveguide system (Juhls et al., 2021; Matsuoka et al., 2021a; Matsuoka et al., 2021b) to derive specific UV absorbance at 254 nm ($SUVA_{254}$). From the absorption and fluorescence measurements described above, $SUVA_{254}$ was calculated as the absorption coefficient at 254 nm normalized to DOC concentration (L mg-C^{-1} m^{-1}). We used the measured humification (HIX) and biological (BIX) indices, as well as PARAFAC components. From the latter, we extracted the following excitation (ex)/emission (em) wavelength pairs (Hansen et al., 2016) : C (340_{ex}:440_{em}), A (260_{ex}:450_{em}), T (275_{ex}:304_{em}), and M peaks (300_{ex}:390_{em}).

2.4. Data Analysis

Spatial interpolation of dissolved and sedimentary REE, DOC, Mn and Fe concentrations was performed using Inverse Distance Weighted (IDW) interpolation in QGIS (v. 3.40.9). To facilitate visual comparison across compartments with different concentration ranges, data were normalized within each compartment (dissolved concentration, sediment) by dividing all values by the compartment-specific maximum concentration, resulting in relative concentrations ranging from 0 to 1.

The following data treatment was performed in R (R. Core Team, 2025). Spearman rank correlations were performed to assess relationships between geochemical variables without assuming linear distributions. Correlations were considered statistically significant at $p < 0.05$. Principal component analysis (PCA) was performed on six variables: dissolved ΣREE, DOC, dissolved Fe, dissolved Mn, $SUVA_{254}$ and temperature. Salinity was not included since it was almost identical for the two sampling seasons. Five variables (REE, DOC, Fe, Mn, $SUVA_{254}$) were tested for normality using Shapiro-Wilk tests. Temperature was not tested for normality as it directly represents the seasonal variations. Variables exhibiting right-skewness (REE: $W = 0.479$, $p < 0.0001$; DOC: $W = 0.865$, $p < 0.0001$; Fe: $W = 0.532$, $p < 0.0001$; Mn: $W = 0.552$, $p < 0.0001$) were $\log_{10}$-transformed (Reimann and Filzmoser, 2000). $SUVA_{254}$ ($W = 0.781$, $p < 0.0001$) and temperature were not transformed. All six variables were z-score standardized, which centers data to a mean of zero and scales to standard deviation of 1. Finally, MANOVA and ANOVA were performed on five variables, excluding temperature as it defines the seasonal grouping, using Pillari's trace as a criterion for seasonal separation. This resulted in biplots with loading vectors scaled ×4 with 95% confidence ellipses.

3. Results

Water temperatures in winter were ~0°C at all stations, while they ranged from 5.6 to 10.6°C ($\bar{x} = 9.0 \pm 1.6$°C) during fall (Lizotte et al., 2023). **Figure 2** illustrates the marked differences in concentrations of dissolved ∑REE between both sampling seasons in the water column (hereafter referred to as overlying water) and porewater. Similar plots for carbon, Fe and Mn data are presented in supporting information (**Figs. A1, A2, and A3** respectively). Although our spatial coverage is admittedly too

https://doi.org/10.5194/egusphere-2026-266
Preprint. Discussion started: 23 January 2026

sparse to allow quantitative interpolation across the Delta, the figure usefully highlights the seasonal contrast in ∑REE concentrations, and the absence of such contrast in the sediment phase, both for ∑REE and carbon. ∑REE concentrations in sediments exhibited minimal seasonal variation, with winter values ranging from 588 µmol kg^{-1} to 1,088 µmol kg^{-1} ($\bar{x}$ = 816 µmol kg^{-1}) and fall values ranging from 591 µmol kg^{-1} to 1,314 µmol kg^{-1} ($\bar{x}$ = 969 µmol kg^{-1}). Similarly, winter carbon concentrations in the sediment ranged between 2.89% and 4.87% ($\bar{x}$ = 3.66%) and fall carbon concentrations ranged between 2.40% and 5.00% ($\bar{x}$ = 3.37%).

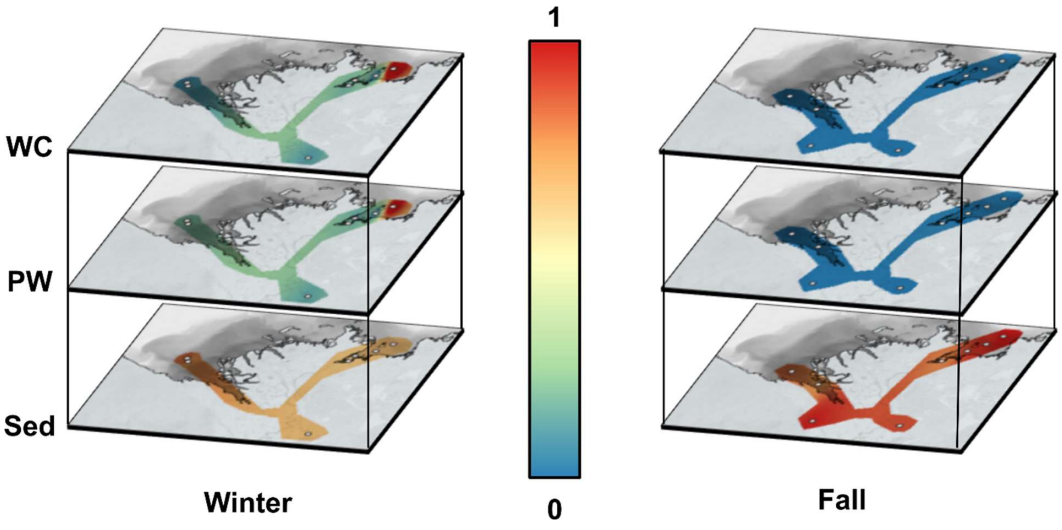

Figure 2: Spatial interpolation of normalized average ΣREE concentrations in the Mackenzie River Delta for the overlying water (water column, WC, top panels), porewater (PW, middle panels) and sediment (Sed, bottom panels) for the winter (left) and fall (right) sampling seasons. Concentrations were normalized for dissolved and solid compartments with the compartment maximum, resulting in relative values between 0 (blue) and 1 (red). Grey circles show sampling sites. (Source: ESRI | Powered by Esri)

In contrast to the sediment, porewater and overlying water samples exhibited strong seasonal trends for both ∑REE and DOC (**Fig. 2, Fig. A1**). To further illustrate the seasonal contrast, we plotted the distribution of concentrations across defined intervals (**Fig. 3**), which shows that winter samples are within the highest concentration ranges for both ∑REE and DOC. These analytes exhibited lower concentrations in fall. During winter, porewater ∑REE concentrations ranged from 2.98 nmol L^{-1} to 1624 nmol L^{-1} ($\bar{x}$ = 217 nmol L^{-1}), and overlying water concentrations ranged from 19.8 nmol L^{-1} to 926 nmol L^{-1} ($\bar{x}$ = 196 nmol L^{-1}). In fall, porewater ∑REE concentrations ranged from 0.26 nmol L^{-1} to 67.96 nmol L^{-1} ($\bar{x}$ = 3.12 nmol L^{-1}) and overlying water concentrations ranged from 0.36 nmol L^{-1} to 0.62 nmol L^{-1} ($\bar{x}$ = 0.50 nmol L^{-1}). This represents a difference of almost two orders of magnitude in average ∑REE concentrations from winter to fall. Similarly, average DOC concentrations are lower by about an order of magnitude in fall compared to winter. In winter, porewater DOC concentrations ranged from

https://doi.org/10.5194/egusphere-2026-266
Preprint. Discussion started: 23 January 2026

13.71 mmol L^{-1} to 58.32 mmol L^{-1} ($\bar{x}$ = 22.66 mmol L^{-1}) and overlying water concentrations ranged from 10.40 mmol L^{-1} to 25.03 mmol L^{-1} ($\bar{x}$ = 19.41 mmol L^{-1}). In comparison, fall concentrations ranged from 0.15 mmol L^{-1} to 20.66 mmol L^{-1} ($\bar{x}$ = 2.86 mmol L^{-1}) for porewater, and from 0.29 mmol L^{-1} to 19.36 mmol L^{-1} ($\bar{x}$ = 6.08 mmol L^{-1}) for overlying water.

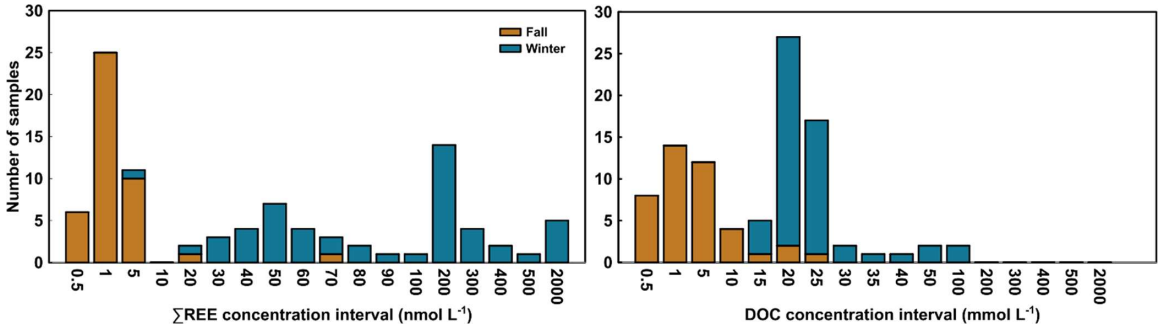

Figure 3: Distribution of samples across logarithmic concentration intervals (n = 48) for ∑REE (mmol L^{-1}) and DOC (mmol L^{-1}) for the winter (blue) and fall (brown) sampling seasons.

Spearman correlation analysis revealed significant relationships in sediment samples for both seasons (**Fig. 4**). In winter sediments, Fe and Mn, Fe and Ce as well as Mn and Ce were positively correlated (**Fig. 4 *a***), while Ce and Nd were strongly positively correlated (**Fig. 4 d**). In the dissolved phase (overlying water and porewater), significant correlations were only found among redox-sensitive metals. Fe and Mn were moderately correlated both in winter and fall (**Fig. 5**) or Ce (**Fig. 5 *b***). Notably, no significant correlations were detected between REE or metals and DOC in either season (**Fig. 5*c-d***). Winter and fall samples form instead distinct clusters based on concentration magnitudes (**Fig. 5c**), with no overlap between seasons. This seasonal separation reflects the approximately two-order-of-magnitude difference in REE concentrations and one-order-of-magnitude difference in DOC concentrations between seasons (**Fig. 2, Fig. A1**). Results from the MANOVA on winter (n=53) and fall (n=36) samples support this (Pillai's trace = 0.883, F-Stat = 125.06, degree of freedom = 5 and p <0.0001). The combination of large effect size (Pillai's trace = 0.883) and high statistical significance indicates that winter and fall samples have distinctly different multivariate profiles across the measured variables. Finally, PCA analysis (**Fig. 6; Tables A1 and A2**) of the porewater Mn, Fe, DOC, ∑REE concentrations, $SUVA_{254}$ and temperature data shows significant multivariate separation, capturing 83% variance in two dimensions.

Finally, $SUVA_{254}$ and HIX indices are higher in the fall than the winter, while values for BIX slightly lower in fall than in winter. The C:T and A:T peak ratios are higher in fall compared to winter, as is the C:M peak ratio, but to a lesser extent than the two other peaks (Table 2).

https://doi.org/10.5194/egusphere-2026-266
Preprint. Discussion started: 23 January 2026

240 **Table 2: Average chromophoric properties of DOM in the water column in the Mackenzie Delta at sampling sites during winter and fall.**

Field season	HIX	$SUVA_{254}$	BIX	C:T	A:T	C:M
Winter	6.0 ± 0.7	1.0 ± 0.8	0.71 ± 0.01	2.5 ± 0.2	4.5 ± 0.3	0.934 ± 0.009
Fall	10 ± 2	2.43 ± 0.08	0.60 ± 0.03	4.0 ± 0.6	7.0 ± 0.8	1.01 ± 0.02

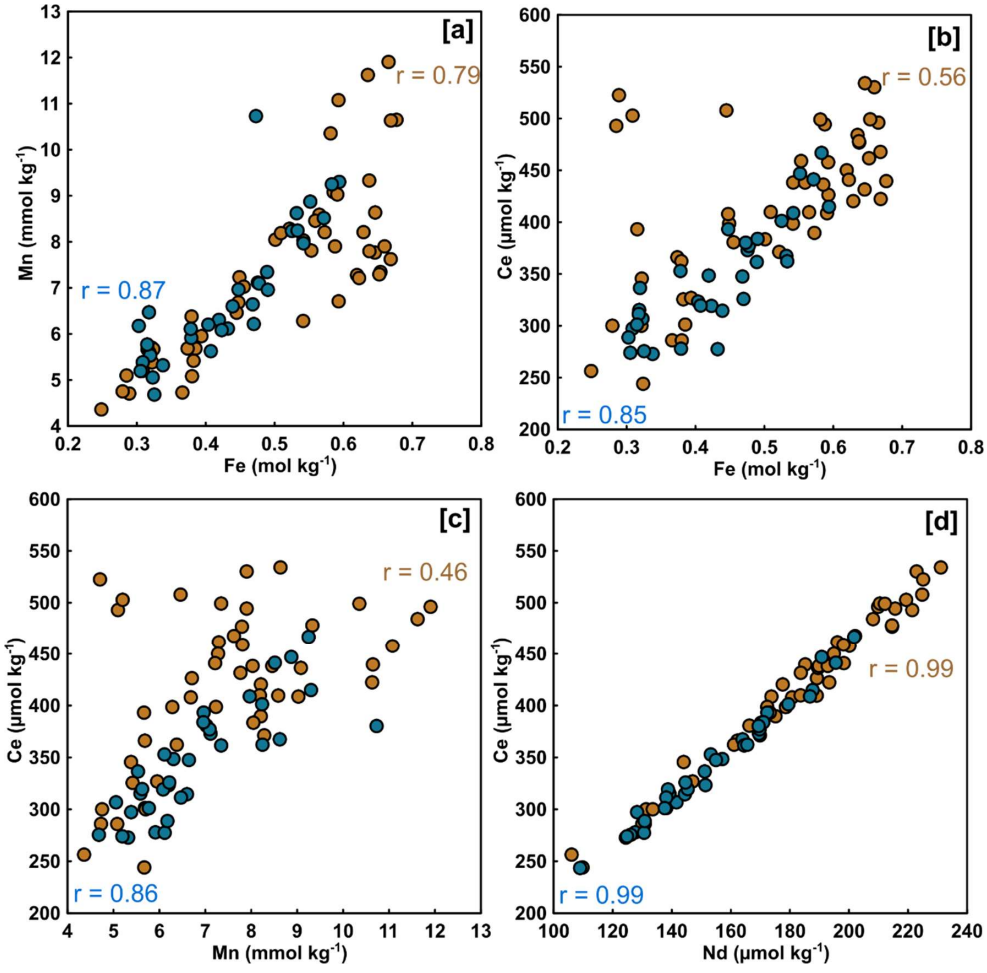

Figure 4: Correlation between solid-phase concentrations of Mn and Fe (*a*), Ce and Fe (*b*), Ce and Mn (*c*), and Ce and Nd (*d*) for the winter (blue) and fall (brown) sampling seasons. Spearman's rank (r) are indicated only for significant correlation ($p < 0.05$).

https://doi.org/10.5194/egusphere-2026-266
Preprint. Discussion started: 23 January 2026

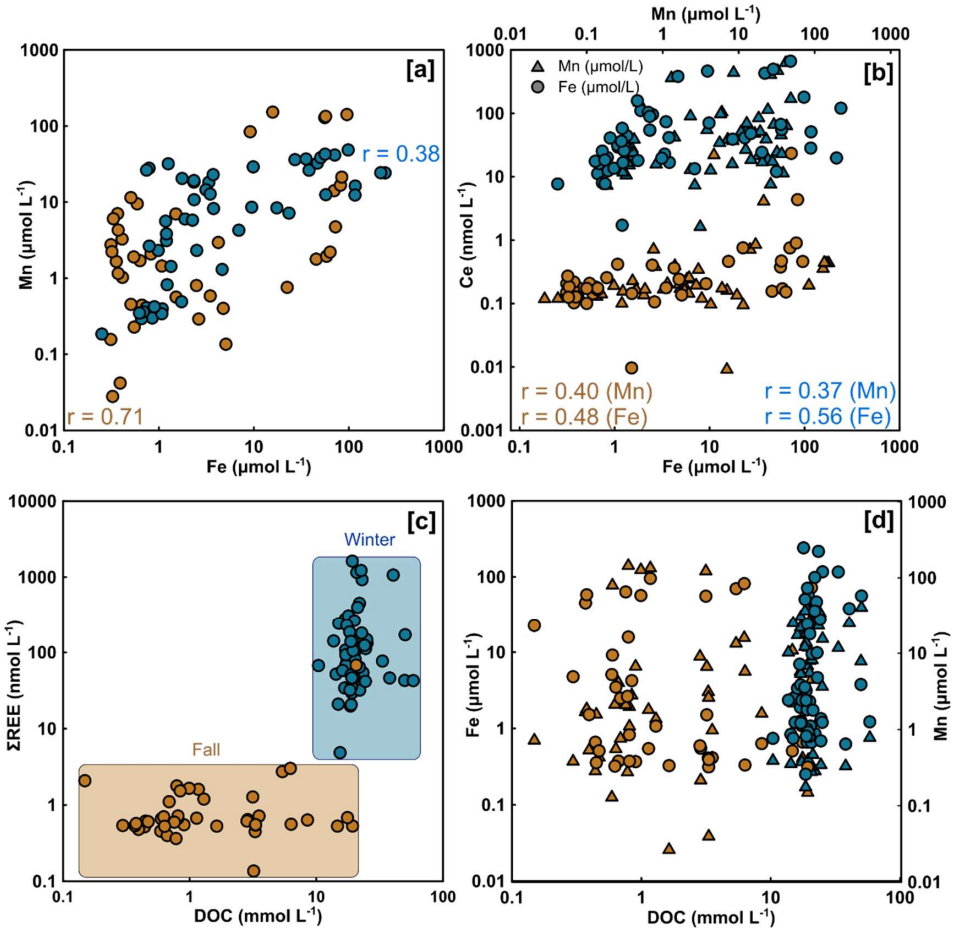

Figure 5: Correlation between porewater Mn and Fe (*a*), Ce, Mn and Fe (*b*), ΣREE and DOC (*c*), and Fe (circles) and Mn (triangles) over DOC (*d*) for the winter (blue) and fall (brown) sampling seasons. Spearman's rank (r) are indicated only for significant correlation ($p < 0.05$). Highlighted zones on panel (c) indicate the two distinct concentration ranges observed between the two sampling seasons.

https://doi.org/10.5194/egusphere-2026-266
Preprint. Discussion started: 23 January 2026

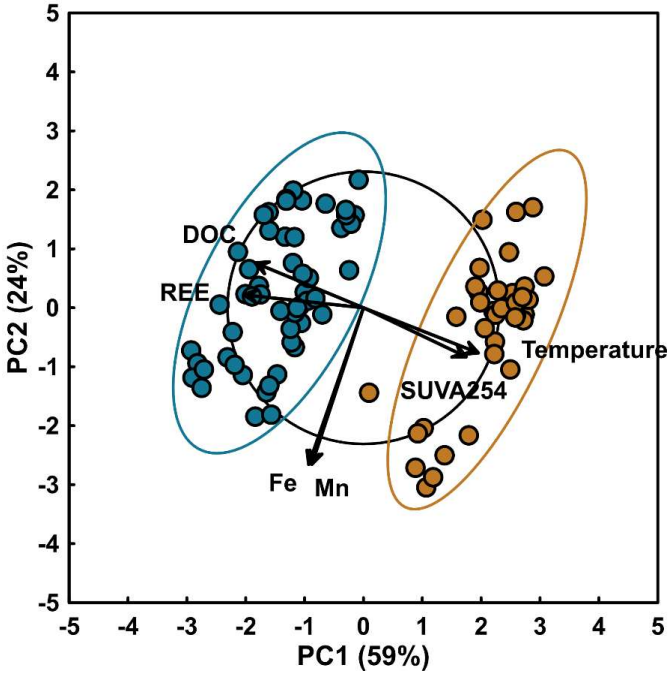

Figure 6: PCA biplot of log-transformed seasonal dissolved Mn, Fe, REE and DOC concentration, as well as $SUVA_{254}$ and temperature data. Points represent individual samples colored by season (winter in blue, *n*=53 and fall in brown, n=36) with 95% confidence ellipses. Arrows indicate variable scaled loadings. Black circle represents the equilibrium descriptor contribution (EDC).

4. Discussion

4.1. Sediment REE stability and Fe-Mn control

Our results show that ∑REE concentrations in the sediments are slightly higher in the fall (816 µmol kg^{-1}) than in the winter (969 µmol kg^{-1}). The strong positive correlations between sediment ∑REE concentrations and redox-sensitive elements (Fe and Mn) (**Fig. 4)** are consistent with Fe and Mn redox-driven recycling controlling REE distribution in the solid phase. Both field (Ye et al., 2019; Toyoda et al., 1990; Takahashi et al., 2015) and laboratory evidence (Bau, 1999) show that REE can be sequestered by Fe and Mn (oxy)hydroxides. The fact that correlation between Fe, Mn and ∑REE in our study are stronger under-ice suggests that near-zero temperatures are particularly favorable for the control of Fe and Mn on REE. Reduced microbial respiration along with the thermal suppression of microbial activity likely create stable conditions near the sediment–water interface (Bouvet et al., 2025; Arnosti et al., 1998) for REE to accumulate onto Fe and Mn (Dang et al., 2022). Covariance between Ce and Nd (**Fig. 4d)** indicates that REE co-vary together, allowing the use of ΣREE concentrations as the key variable in this study.

https://doi.org/10.5194/egusphere-2026-266
Preprint. Discussion started: 23 January 2026

4.2. Dissolved Organic Matter Quantity *versus* Quality in REE Complexation

Porewater and overlying water (i.e., water-column) dissolved ∑REE concentration data shows a seasonal trend (**Fig. 2 and Fig. 3**), with two distinct populations of porewater ∑REE and DOC measurements (F-statistics of 409.13 and 220.09 respectively, p-values < 0.0001; **Table A4**) (**Fig. 5c)**. PCA shows that DOC and ∑REE co-vary along the PC1 axis (59% variance), inversely correlated with temperature and $SUVA_{254,}$ due to the 180º angle between these vectors. Meanwhile, Fe and Mn co-vary along PC2, independently of the temperature, DOC concentrations and DOM quality or of ∑REE concentrations, given the 90º separation between the vectors. This seasonal variability, where REE and DOC co-vary and are inversely related to temperature and DOM aromaticity ($SUVA_{254}$), is consistent with OM complexation of REE during colder periods being controlled by DOM quantity. The second principal component (PC2) explain the next largest variance, which likely captures the redox processes that control the mobilization of Fe and Mn, independent of seasonal effects. This finding aligns with recent work in the sub-arctic George River, Canada (Marginson et al., 2024) and the temperate Sleepers River, USA, in which dissolved water-column REE and DOC exhibited positive correlations (Norton and Shanley, 2025). Seasonal variability in REE dynamics in rivers has also been evidenced for tropical systems, where dissolved REE concentrations showed strong seasonal variation driven by watershed runoff during wet seasons versus scavenging by organic-rich particles during dry seasons (Dang et al., 2023). While our Arctic system operates under different temperatures and biological productivity regimes, both studies demonstrate that seasonal changes in organic matter quality and quantity influence dissolved REE dynamics in river systems with pronounced seasonal variability. Several studies point to organic matter quality playing a crucial role in REE complexation and distribution in aquatic systems (Catrouillet et al., 2020; Pourret et al., 2007c; Marsac et al., 2021; Tadayon et al., 2024). Overall, it is generally accepted that complexed REE account for up to 95% of the dissolved phase in freshwater (Tang and Johannesson, 2003; Johannesson et al., 1995; Pourret et al., 2007b; Revel et al., 2025).

The strong seasonal contrast in DOC concentration (Fig. 2) can be investigated in the light of the chromophoric properties of DOM, namely low $SUVA_{254}$ and HIX values in the winter relative to the fall (Table 2). Those values point to winter OM samples having a lower aromaticity and a lower proportion of humic acid than the fall sample (Hansen et al., 2016). Similarly, BIX values point to a higher proportion of autochthonous dissolved organic matter in the winter and the C:T, A:T and C:M peak-ratios point to a lower humic character in winter. Collectively, those indicators of autochthonous DOM in the winter are consistent with the enzymatic breakdown of solid-phase OM to aqueous DOM maintaining a significant activity at low temperatures (Davidson et al., 2006), while the subsequent mineralization of aqueous DOM remains inhibited. This differential temperature sensitivity may explain in DOM accumulation in the porewater in the winter (German et al., 2012; Schädel et al., 2016). This lower winter OM degradation is consistent with the markedly lower bacterial abundance observed in winter samples compared to fall samples for the Mackenzie Delta (Lizotte et al., 2023). In fall, increased DOM degradation in the porewater suppresses the autochthonous signal, leaving catchment-derived terrestrial DOM. The shift in DOM character between seasons likely extends to molecular weight distributions, with autochthonous winter DOM, characterized by enzymatic breakdown products, typically exhibiting lower molecular weight compared to the terrestrial, humic-rich DOM

https://doi.org/10.5194/egusphere-2026-266
Preprint. Discussion started: 23 January 2026

observed in fall (Hansen et al. 2016). However, the literature present conflicting evidence regarding the role of molecular weight in REE complexation, with some studies showing that REE generally preferentially complex with high molecular weight OM (Tang and Johannesson, 2003; Catrouillet et al., 2020; Tang and Johannesson, 2010), and others preferentially complex with low molecular weight OM (Zilber et al., 2024). Without size fractionation data, we cannot evaluate which mechanism dominates in our system.

Thus, we find two distinct porewater DOM pools depending on the season. Despite fall DOM having higher-affinity (Marsac et al., 2011) binding sites (phenolic groups, binding constant (logarithm of the stability constant (K) for the complexation reaction, log K, = 4.93) compared to winter DOM (carboxylic groups, log K = 3.29), dissolved REE concentrations are lower in fall. This likely reflects the dominance of DOC concentration over binding site quality, that is, the winter higher DOC concentrations (Fig. 2) provide sufficient low-affinity sites to complex more ∑REE than the limited pool of high-affinity sites available in fall.

The seasonal variations in organic matter quantity and quality observed in the Mackenzie Delta parallel those documented in the Lena Delta, another major Arctic river system (Juhls et al., 2020). In both systems, winter DOM is characterized by older, more degraded material with reduced overall fluxes. These seasonal organic matter dynamics are particularly important because coastal environments and deltas serve as crucial carbon reservoirs and processing hotspots (Bianchi and Allison, 2009), collectively accounting for approximately 80% of total marine carbon burial (Hedges and Keil, 1995). This significant contribution results from high sedimentation rates and proximity to continental organic matter sources (Bianchi et al., 2018; Goñi et al., 2000). Recent modeling work on the Mackenzie River plume demonstrated that seasonal variations in terrestrial CDOM export affect coastal light attenuation, phytoplankton phenology, and sea-surface temperature, switching the coastal zone from a CO_2 sink to a source (Bertin et al., 2025). We note that logistical constraints resulted in partially non-overlapping sampling locations between seasons, particularly in the western transect. However, eastern sites were sampled at identical locations in both seasons and confirm the winter enrichment pattern, while the complete separation of seasonal samples in multivariate space (Fig. 6) demonstrates that season-driven processes dominate over site-specific spatial variability. Our findings that seasonal dynamics shapes REE–organic matter interactions therefore have broader implications for understanding coupled carbon-trace element cycling in these biogeochemical hotspots.

4.3. Inorganic Controls on Dissolved REE Mobility

Temperature is a potential factor controlling REE release from the sediment to the porewater. Marginson et al. (2024) documented a significant correlation between lower temperatures and elevated REE concentrations in the George and Koroc Rivers, in their tributaries, and in thermokarst lakes in northern Québec. Their proposed mechanism invokes a higher partial pressure of CO_2 in colder waters (Young et al., 2025) which subsequently increases the formation and stability of REE–carbonate complexes in solution (Marginson et al., 2024). Our results are consistent with this previous report.

Competition from dissolved Fe and Mn for DOM binding sites (Tang and Johannesson, 2003; Pourret et al., 2007b; Marsac et al., 2011; Neweshy et al., 2022) likely amplifies the observed higher ∑REE concentrations. During summer, the season of high

https://doi.org/10.5194/egusphere-2026-266
Preprint. Discussion started: 23 January 2026

biological productivity and of high microbial respiration, soluble Fe^{2+} produced via the reductive dissolution of Fe (oxy)hydroxides accumulates to levels that have been shown to displace REE from DOM binding sites (Neweshy et al., 2022). Indeed, Fe^{3+}, Fe^{2+} and Mn^{2+} all have binding constants (pK_{MHA} for humic acid of respectively 0.8, 2.1 and 3.4) that are similar to that of REE (average pK_{MHA} for humic acid of 1.53) (Tang and Johannesson, 2003), with Fe acting as one of the most important competitors to REE in complexation by DOC (Takahashi et al., 1997). DOM ligands control most of the mobilization of REE from solid to dissolved phase in natural waters (Wen et al., 2024). The increased competition for DOM ligands may thus partly explain the lower dissolved ∑REE concentrations, leaving in solution the poorly soluble free REE^{3+} ions or carbonate complexes (Tang and Johannesson, 2003; Johannesson et al., 1995; Pourret et al., 2007b).

5. Conclusion

Our study reveals the sensitivity of REE cycling to seasonal environmental changes in Arctic coastal systems. Sedimentary ∑REE concentrations remain remarkably stable across seasons, with positive correlations to Fe and Mn (oxy)hydroxides that strengthen in winter. In contrast, porewater ∑REE concentrations exhibit pronounced seasonal variability, with significantly higher values in winter than in fall. This seasonal contrast tracks DOC concentrations, indicating that variations in DOM quantity play a stronger role in controlling REE mobility than changes in DOM quality alone. Winter DOM is characterized by lower aromaticity and molecular weight and weaker complexation capacity, but is found in much greater abundance, whereas fall DOM, enriched in humic substances and aromatic compounds, offers stronger ligands for REE binding but in much lower concentrations. Colder winter conditions likely enhancing the stability of REE–carbonate complexes and suppress microbial degradation of organic matter, both of which contribute to elevated REE concentrations. In contrast, warmer summer temperatures accelerate organic matter degradation, lowering dissolved ligand abundance and reducing REE solubility. These seasonal dynamics have implications for understanding REE transport in Arctic coastal systems, which are experiencing intensifying riverine influence as warming accelerates (Emmerton et al., 2008b; Opsahl et al., 1999; Kipp et al., 2020).

https://doi.org/10.5194/egusphere-2026-266
Preprint. Discussion started: 23 January 2026

Appendix A

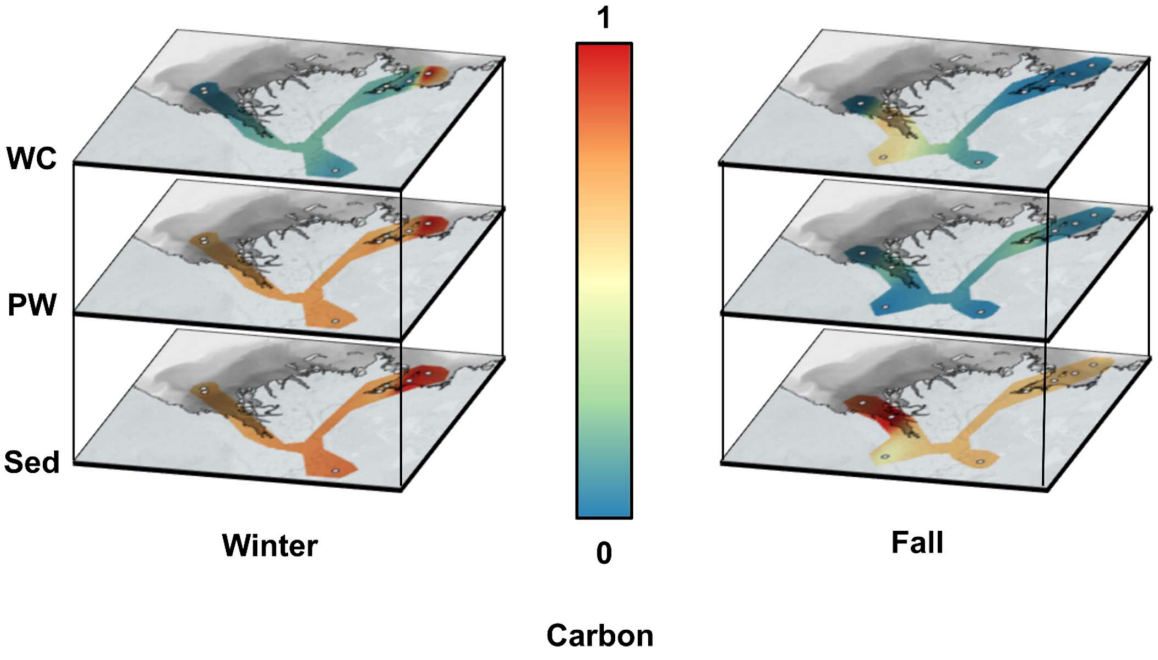

Figure A1: Spatial interpolation of normalized average carbon concentrations in the Mackenzie River Delta for the overlying water (water column, WC, top panels), porewater (PW, middle panels) and sediment (Sed, bottom panels) for the winter (left) and fall (right) sampling seasons. Concentrations were normalized for dissolved and solid compartments with the compartment maximum, resulting in relative values between 0 (blue) and 1 (red). Grey circles show sampling sites. (Source: ESRI | Powered by Esri)

https://doi.org/10.5194/egusphere-2026-266
Preprint. Discussion started: 23 January 2026

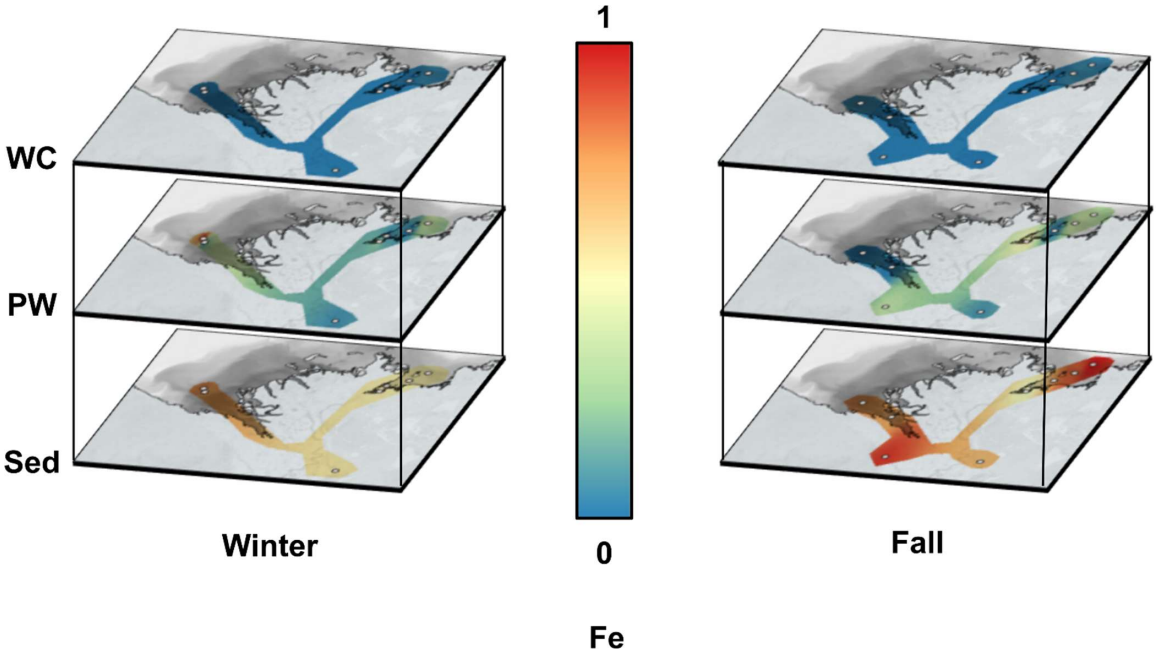

Figure A2: Spatial interpolation of normalized average Fe concentrations in the Mackenzie River Delta for the overlying water (water column, WC, top panels), porewater (PW, middle panels) and sediment (Sed, bottom panels) for the winter (left) and fall (right) sampling seasons. Concentrations were normalized for dissolved and solid compartments with the compartment maximum, resulting in relative values between 0 (blue) and 1 (red). Grey circles show sampling sites. (Source: ESRI | Powered by Esri)

https://doi.org/10.5194/egusphere-2026-266
Preprint. Discussion started: 23 January 2026

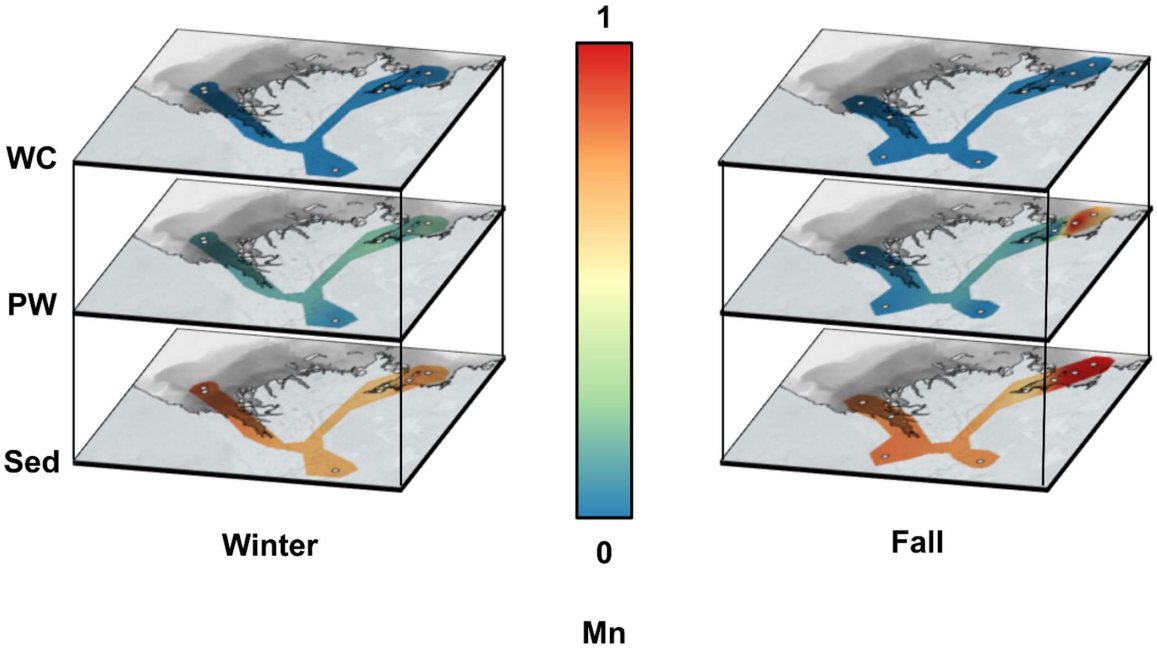

Figure A3: Spatial interpolation of normalized average Mn concentrations in the Mackenzie River Delta for the overlying water (water column, WC, top panels), porewater (PW, middle panels) and sediment (Sed, bottom panels) for the winter (left) and fall (right) sampling seasons. Concentrations were normalized for dissolved and solid compartments with the compartment maximum, resulting in relative values between 0 (blue) and 1 (red). Grey circles show sampling sites. (Source: ESRI | Powered by Esri)

Table A1 Principal component analysis summary of log-transformed seasonal dissolved Mn, Fe, REE and DOC data, $SUVA_{254}$ and temperature data for winter (n=53) and fall (n=36).

Component	Eigenvalue	Variance_Percent	Cumulative_Percent
PC1	3.540779	59.01298	59.01298
PC2	1.438984	23.98306	82.99605
PC3	0.398984	6.649732	89.64578
PC4	0.360994	6.016569	95.66235
PC5	0.182051	3.034179	98.69653
PC6	0.078208	1.303474	100

https://doi.org/10.5194/egusphere-2026-266
Preprint. Discussion started: 23 January 2026

Table A2 Principal component variable loadings of seasonal dissolved Mn, Fe, REE and DOC data, $SUVA_{254}$ and temperature data for winter (n=53) and fall (n=36).

Variable	PC1	PC2	PC3	PC4
REE_log	-0.50833	0.054846	-0.20157	-0.07961
DOC_log	-0.46	0.190304	-0.17919	0.555992
Fe_log	-0.23202	-0.66391	-0.55114	-0.35446
Mn_log	-0.21909	-0.66348	0.615679	0.348132
Temperature	0.487757	-0.19134	0.072649	-0.14759
SUVA254	0.436185	-0.20783	-0.48905	0.644914

Table A3 MANOVA test for differences between winter (n=53) and fall (n=36).

Statistical Test	Value	F-Statistic	df	p-value
Pillai's trace	0.883	125.06	(5,83)	< 0.0001

Table A4 Univariate ANOVA of seasonal dissolved Mn, Fe, REE and DOC data and $SUVA_{254}$ data for winter (n=53) and fall (n=36).

Variable	df	F-statistic	p-value	Partial n^2
REE_log	1, 87	409.13	< 0.0001	0.825
DOC_log	1, 87	220.09	< 0.0001	0.717
Fe_log	1, 87	3.45	0.067	0.038
Mn_log	1, 87	2.83	0.096	0.032
SUVA254	1, 87	107.17	< 0.0001	0.552

https://doi.org/10.5194/egusphere-2026-266
Preprint. Discussion started: 23 January 2026

Data availability

Concentrations of elements in porewater and sediment are available on Borealis at DOI:10.5683/SP3/MLSXCK (Bossé-Demers et al., 2026). Water column DOM proprieties are available on Pangaea at DOI: 10.1594/PANGAEA.937587 (Juhls et al., 2021)

CRediT authorship contribution statement

Thomas Bossé-Demers: Writing – original draft, Methodology, Investigation, Conceptualization. Bennet Juhls: Writing – review & editing, Resources. Martine Lizotte: Writing – review & editing, Resources, Conceptualization. Santiago Mareque: Writing – review & editing. Audrey Gaudy: Investigation. Raoul-Marie Couture: Writing – review & editing, Writing – original draft, Validation, Supervision, Project administration, Methodology, Investigation, Funding acquisition, Formal analysis, Conceptualization.

Competing interests

The authors declare that they have no conflict of interest.

Acknowledgements

We thank the community members of Aklavik, Inuvik and Tuktoyaktuk for their support in the planning and execution of this project. We are thankful to L. Oziel for his devoted help with sampling in the Mackenzie Delta and A. Matsuoka for help with mission logistics. We acknowledge funding from the Horizon Europe Research and Innovation Program Nunataryuk project (grant #773421). RMC was funded by the Natural Sciences and Engineering Research Council of Canada (NSERC) through the Discovery Grant program and the Sentinel North program of Université Laval, Canada First Research Excellence Funds. BJ was funded by the European Space Agency (ESA) as part of the Climate Change Initiative (CCI) fellowship (ESA ESRIN/Contract No. 4000l3376l/2l/I-NB) and the BNP Paribas Foundation with the project “FLO CHAR.” We thank C. Dalencourt, D. Larivière, S. Groleau and C. Beaulieu for help with instrumental analysis. We thank M. Thaler for editing the manuscript.

https://doi.org/10.5194/egusphere-2026-266
Preprint. Discussion started: 23 January 2026

References

Abbott, A. N., Haley, B. A., McManus, J., and Reimers, C. E.: The sedimentary flux of dissolved rare earth elements to the ocean, Geochimica Et Cosmochimica Acta, 154, 186-200, 10.1016/j.gca.2015.01.010, 2015.

Abdul Aziz, O. I. and Burn, D. H.: Trends and variability in the hydrological regime of the Mackenzie River Basin, Journal of Hydrology, 319, 282-294, 10.1016/j.jhydrol.2005.06.039, 2006.

Alonso, E., Sherman, A. M., Wallington, T. J., Everson, M. P., Field, F. R., Roth, R., and Kirchain, R. E.: Evaluating rare earth element availability: a case with revolutionary demand from clean technologies, Environ Sci Technol, 46, 3406-3414, 10.1021/es203518d, 2012.

Arnosti, C., Jørgensen, B. B., Sagemann, J., and Thamdrup, B.: Temperature dependence of microbial degradation of organic matter in marine sediments: polysaccharide hydrolysis, oxygen consumption, and sulfate reduction, Marine Ecology Progress Series, 165, 59-70, 10.3354/meps165059, 1998.

Bertin, C., Le Fouest, V., Carroll, D., Dutkiewicz, S., Menemenlis, D., Matsuoka, A., Manizza, M., and Miller, C. E.: Colored dissolved organic matter (CDOM) alters the seasonal physics and biogeochemistry of the Arctic Mackenzie River plume, Biogeosciences, 22, 6607-6629, 10.5194/bg-22-6607-2025, 2025.

Bertin, C., Carroll, D., Menemenlis, D., Dutkiewicz, S., Zhang, H., Matsuoka, A., Tank, S., Manizza, M., Miller, C. E., Babin, M., Mangin, A., and Le Fouest, V.: Biogeochemical River Runoff Drives Intense Coastal Arctic Ocean CO2 Outgassing, Geophysical Research Letters, 50, 10.1029/2022gl102377, 2023.

Bossé-Demers, T., Juhls, B., Lizotte, M., Mareque, S., Gaudy, A., and Couture, R.: Elements concentrations for "Seasonal Contrast in Rare Earth Elements Concentration in Sediment of the Mackenzie Delta" (V1), Borealis [dataset], doi:10.5683/SP3/MLSXCK, 2026.

Bossé-Demers, T., Gobeil, C., Juhls, B., Lizotte, M., Fritz, M., Bröder, L., Matsuoka, A., Mareque, S., and Couture, R.-M.: Distribution of rare earth elements and their signatures from the Mackenzie River delta to the abyssal Arctic Ocean, Continental Shelf Research, 289, 105464, 10.1016/j.csr.2025.105464, 2025.

Bouvet, C., Beauregard, P. B., and Guéguen, C.: Low-temperature biodegradation of freshwater dissolved organic matter during winter-to-spring transition, Frontiers in Environmental Science, 12, 10.3389/fenvs.2024.1524626, 2025.

Catrouillet, C., Guenet, H., Pierson-Wickmann, A.-C., Dia, A., LeCoz, M. B., Deville, S., Lenne, Q., Suko, Y., and Davranche, M.: Rare earth elements as tracers of active colloidal organic matter composition, Environmental Chemistry, 17, 133-139, 10.1071/EN19159, 2020.

Dang, D. H., Ha, Q. K., Némery, J., and Strady, E.: The seasonal variations in the interactions between rare earth elements and organic matter in tropical rivers, Chemical Geology, 638, 121711, 10.1016/j.chemgeo.2023.121711, 2023.

Dang, D. H., Wang, W., Sikma, A., Chatzis, A., and Mucci, A.: The contrasting estuarine geochemistry of rare earth elements between ice-covered and ice-free conditions, Geochimica et Cosmochimica Acta, 317, 488-506, 10.1016/j.gca.2021.10.025, 2022.

https://doi.org/10.5194/egusphere-2026-266
Preprint. Discussion started: 23 January 2026

Davidson, E. A., Janssens, I. A., and Luo, Y. Q.: On the variability of respiration in terrestrial ecosystems:: moving beyond, Global Change Biology, 12, 154-164, 10.1111/j.1365-2486.2005.01065.x, 2006.

Davranche, M., Pourret, O., Gruau, G., and Dia, A.: Impact of humate complexation on the adsorption of REE onto Fe oxyhydroxide, J Colloid Interface Sci, 277, 271-279, 10.1016/j.jcis.2004.04.007, 2004.

DeGrandpre, E. L., DeGrandpre, M. D., Colman, B. P., and Valett, H. M.: Observations of River Solute Concentrations during Ice Formation, ACS ES&T Water, 1, 1695-1701, 10.1021/acsestwater.1c00064, 2021.

Deng, K., Yang, S., Du, J., Lian, E., and Vance, D.: Dominance of benthic flux of REEs on continental shelves: implications for oceanic budgets, Geochemical Perspectives Letters, 22, 26-30, 10.7185/geochemlet.2223, 2022.

Emmerton, C. A., Lesack, L. F. W., and Vincent, W. F.: Mackenzie River nutrient delivery to the Arctic Ocean and effects of the Mackenzie Delta during open water conditions, Global Biogeochemical Cycles, 22, 10.1029/2006gb002856, 2008a.

Emmerton, C. A., Lesack, L. F. W., and Vincent, W. F.: Nutrient and organic matter patterns across the Mackenzie River, estuary and shelf during the seasonal recession of sea-ice, Journal of Marine Systems, 74, 741-755, 10.1016/j.jmarsys.2007.10.001, 2008b.

Finlay, J., Neff, J., Zimov, S., Davydova, A., and Davydov, S.: Snowmelt dominance of dissolved organic carbon in high-latitude watersheds: Implications for characterization and flux of river DOC, Geophysical Research Letters, 33, 10.1029/2006GL025754, 2006.

Gareis, J. A. L. and Lesack, L. F. W.: Fluxes of particulates and nutrients during hydrologically defined seasonal periods in an ice-affected great Arctic river, the Mackenzie, Water Resour. Res., 53, 6109-6132, 10.1002/2017WR020623, 2017.

German, D. P., Marcelo, K. R. B., Stone, M. M., and Allison, S. D.: The Michaelis–Menten kinetics of soil extracellular enzymes in response to temperature: a cross-latitudinal study, Global Change Biology, 18, 1468-1479, 10.1111/j.1365-2486.2011.02615.x, 2012.

Goñi, M. A., Yunker, M. B., Macdonald, R. W., and Eglinton, T. I.: Distribution and sources of organic biomarkers in arctic sediments from the Mackenzie River and Beaufort Shelf, Marine Chemistry, 71, 23-51, 10.1016/s0304-4203(00)00037-2, 2000.

Grenier, M., Brown, K. A., Colombo, M., Belhadj, M., Baconnais, I., Pham, V., Soon, M., Myers, P. G., Jeandel, C., and François, R.: Controlling factors and impacts of river-borne neodymium isotope signatures and rare earth element concentrations supplied to the Canadian Arctic Archipelago, Earth and Planetary Science Letters, 578, 10.1016/j.epsl.2021.117341, 2022.

Gudasz, C., Bastviken, D., Steger, K., Premke, K., Sobek, S., and Tranvik, L. J.: Temperature-controlled organic carbon mineralization in lake sediments, Nature, 466, 478-481, 10.1038/nature09186, 2010.

Guo, H., Tuduri, J., Nabyl, Z., Erdmann, S., Li, X., and Gaillard, F.: Rare earth elements in apatite: A proxy for unravelling carbonatite melt compositions, Earth and Planetary Science Letters, 642, 118863, 10.1016/j.epsl.2024.118863, 2024.

Hansen, A. M., Kraus, T. E. C., Pellerin, B. A., Fleck, J. A., Downing, B. D., and Bergamaschi, B. A.: Optical properties of dissolved organic matter (DOM): Effects of biological and photolytic degradation, Limnology and Oceanography, 61, 1015-1032, 10.1002/lno.10270, 2016.

https://doi.org/10.5194/egusphere-2026-266
Preprint. Discussion started: 23 January 2026

Haque, N., Hughes, A., Lim, S., and Vernon, C.: Rare Earth Elements: Overview of Mining, Mineralogy, Uses, Sustainability and Environmental Impact, Resources-Basel, 3, 614-635, 10.3390/resources3040614, 2014.

Hill, P. R., Lewis, C. P., Desmarais, S., Kauppaymuthoo, V., and Rais, H.: The Mackenzie Delta: sedimentary processes and facies of a high-latitude, fine-grained delta, Sedimentology, 48, 1047-1078, 10.1046/j.1365-3091.2001.00408.x, 2001.

Holmes, R. M., McClelland, J. W., Peterson, B. J., Shiklomanov, I. A., Shiklomanov, A. I., Zhulidov, A. V., Gordeev, V. V., and Bobrovitskaya, N. N.: A circumpolar perspective on fluvial sediment flux to the Arctic Ocean, Global Biogeochemical Cycles, 16, 45-41-45-14, 10.1029/2001gb001849, 2002.

Holmes, R. M., McClelland, J. W., Peterson, B. J., Tank, S. E., Bulygina, E., Eglinton, T. I., Gordeev, V. V., Gurtovaya, T. Y., Raymond, P. A., Repeta, D. J., Staples, R., Striegl, R. G., Zhulidov, A. V., and Zimov, S. A.: Seasonal and Annual Fluxes of Nutrients and Organic Matter from Large Rivers to the Arctic Ocean and Surrounding Seas, Estuaries and Coasts, 35, 369-382, 10.1007/s12237-011-9386-6, 2012.

Jermilova, U., Kirk, J. L., Moe, S. J., Landis, W. G., Sharpe, E., McGovern, M., Braaten, H. F. V., Gundersen, C. B., Dastoor, A. P., Schaefer, K., and Hintelmann, H. H.: Assessing mercury exposure to water and fish of the Mackenzie watershed using a Bayesian network analysis, Integrated Environmental Assessment and Management, 21, 396-413, 10.1093/inteam/vjae011, 2025.

Johannesson, K. H., Lyons, W. B., Stetzenbach, K. J., and Byrne, R. H.: The Solubility Control of Rare Earth Elements in Natural Terrestrial Waters and the Significance of PO and CO in Limiting Dissolved Rare Earth Concentrations: A Review of Recent Information, Aquatic Geochemistry, 1, 157-173, 10.1007/Bf00702889, 1995.

Juhls, B., Stedmon, C. A., Morgenstern, A., Meyer, H., Hölemann, J., Heim, B., Povazhnyi, V., and Overduin, P. P.: Identifying Drivers of Seasonality in Lena River Biogeochemistry and Dissolved Organic Matter Fluxes, Frontiers in Environmental Science, 8, 10.3389/fenvs.2020.00053, 2020.

Juhls, B., Matsuoka, A., Lizotte, M., Bécu, G., Overduin, P. P., El Kassar, J., Devred, E., Doxaran, D., Ferland, J., Forget, M. H., Hilborn, A., Hieronymi, M., Leymarie, E., Maury, J., Oziel, L., Tisserand, L., Anikina, D. O. J., Dillon, M., and Babin, M.: Seasonal dynamics of dissolved organic matter in the Mackenzie Delta, Canadian Arctic waters: Implications for ocean colour remote sensing, Remote Sensing of Environment, 283, 10.1016/j.rse.2022.113327, 2022.

Juhls, B., Lizotte, M., Matsuoka, A., Mével, G., Bécu, G., Overduin, P. P., Devred, E., Doxaran, D., Ferland, J., Forget, M.-H., Hilborn, A., Leymarie, E., Maury, J., Oziel, L., Tisserand, L., Miles, D., Anikina, D. O. J., Guilmette, C., Béguin, M., Couture, R.-M., Bossé-Demers, T., Laberge-Carignan, A., Chaillou, G., Bélanger, S., Bruyant, F., and Babin, M.: Hydrographical, biogeochemical and biooptical water properties in the Mackenzie Delta Region during 4 expeditions from spring to fall in 2019, 10.1594/PANGAEA.937587, 2021.

Kipp, L. E., Henderson, P. B., Wang, Z. A., and Charette, M. A.: Deltaic and Estuarine Controls on Mackenzie River Solute Fluxes to the Arctic Ocean, Estuaries and Coasts, 43, 1992-2014, 10.1007/s12237-020-00739-8, 2020.

Kopec, B. G., Klein, E. S., Feldman, G. C., Pedron, S. A., Bailey, H., Causey, D., Hubbard, A., Marttila, H., and Welker, J. M.: Arctic Freshwater Sources and Ocean Mixing Relationships Revealed With Seawater Isotopic Tracing, Journal of Geophysical Research: Oceans, 129, e2023JC020583, 10.1029/2023JC020583, 2024.

https://doi.org/10.5194/egusphere-2026-266
Preprint. Discussion started: 23 January 2026

Landy, J. C., Dawson, G. J., Tsamados, M., Bushuk, M., Stroeve, J. C., Howell, S. E. L., Krumpen, T., Babb, D. G., Komarov, A. S., Heorton, H. D. B. S., Belter, H. J., and Aksenov, Y.: A year-round satellite sea-ice thickness record from CryoSat-2, Nature, 609, 517-522, 10.1038/s41586-022-05058-5, 2022.

Leitch, D. R., Carrie, J., Lean, D., Macdonald, R. W., Stern, G. A., and Wang, F.: The delivery of mercury to the Beaufort Sea of the Arctic Ocean by the Mackenzie River, Sci Total Environ, 373, 178-195, 10.1016/j.scitotenv.2006.10.041, 2007.

Liu, S., Wang, P., Huang, Q., Yu, J., Pozdniakov, S. P., and Kazak, E. S.: Seasonal and spatial variations in riverine DOC exports in permafrost-dominated Arctic river basins, Journal of Hydrology, 612, 128060, 10.1016/j.jhydrol.2022.128060, 2022.

Lizotte, M., Juhls, B., Matsuoka, A., Massicotte, P., Mével, G., Anikina, D. O. J., Antonova, S., Bécu, G., Béguin, M., Bélanger, S., Bossé-Demers, T., Bröder, L., Bruyant, F., Chaillou, G., Comte, J., Couture, R.-M., Devred, E., Deslongchamps, G., Dezutter, T., Dillon, M., Doxaran, D., Flamand, A., Fell, F., Ferland, J., Forget, M.-H., Fritz, M., Gordon, T. J., Guilmette, C., Hilborn, A., Hussherr, R., Irish, C., Joux, F., Kipp, L., Laberge-Carignan, A., Lantuit, H., Leymarie, E., Mannino, A., Maury, J., Overduin, P., Oziel, L., Stedmon, C., Thomas, C., Tisserand, L., Tremblay, J.-É., Vonk, J., Whalen, D., and Babin, M.: Nunataryuk field campaigns: understanding the origin and fate of terrestrial organic matter in the coastal waters of the Mackenzie Delta region, Earth System Science Data, 15, 1617-1653, 10.5194/essd-15-1617-2023, 2023.

Macdonald, R. W., Paton, D. W., Carmack, E. C., and Omstedt, A.: The freshwater budget and under-ice spreading of Mackenzie River water in the Canadian Beaufort Sea based on salinity and 18O/16O measurements in water and ice, Journal of Geophysical Research: Oceans, 100, 895-919, 10.1029/94jc02700, 2012.

MacMillan, G. A., Chetelat, J., Heath, J. P., Mickpegak, R., and Amyot, M.: Rare earth elements in freshwater, marine, and terrestrial ecosystems in the eastern Canadian Arctic, Environ Sci Process Impacts, 19, 1336-1345, 10.1039/c7em00082k, 2017.

Marginson, H., MacMillan, G. A., Wauthy, M., Sicaud, E., Gérin-Lajoie, J., Dedieu, J. P., and Amyot, M.: Drivers of rare earth elements (REEs) and radionuclides in changing subarctic (Nunavik, Canada) surface waters near a mining project, J. Hazard. Mater., 471, 134418, 10.1016/j.jhazmat.2024.134418, 2024.

Marsac, R., Davranche, M., Gruau, G., Bouhnik-Le Coz, M., and Dia, A.: An improved description of the interactions between rare earth elements and humic acids by modeling: PHREEQC-Model VI coupling, Geochimica Et Cosmochimica Acta, 75, 5625-5637, 10.1016/j.gca.2011.07.009, 2011.

Marsac, R., Catrouillet, C., Davranche, M., Bouhnik-Le Coz, M., Briant, N., Janot, N., Otero-Fariña, A., Groenenberg, J. E., Pédrot, M., and Dia, A.: Modeling rare earth elements binding to humic acids with model VII, Chemical Geology, 567, 10.1016/j.chemgeo.2021.120099, 2021.

Matsuoka, A., Juhls, B., Bécu, G., Oziel, L., Leymarie, E., Lizotte, M., Ferland, J., Béguin, M., Laberge-Carignan, A., Guilmette, C., Maury, J., Hilborn, A., Tisserand, L., Devred, E., Doxaran, D., Bossé-Demers, T., and Babin, M.: Colored dissolved organic matter absorption (aCDOM) and spectal slopes (S) in the surface water of the Mackenzie Delta Region during 4 expeditions from spring to fall in 2019, PANGAEA [dataset], 10.1594/PANGAEA.937580, 2021a.

Matsuoka, A., Juhls, B., Bécu, G., Oziel, L., Leymarie, E., Lizotte, M., Ferland, J., Béguin, M., Laberge-Carignan, A., Guilmette, C., Maury, J., Hilborn, A., Tisserand, L., Devred, E., Doxaran, D., Bossé-Demers, T., Gonçalves-Araujo, R., Stedmon, C. A., and Babin, M.: Fluorescent dissolved organic matter

https://doi.org/10.5194/egusphere-2026-266
Preprint. Discussion started: 23 January 2026

(FDOM) intensity (Parafac components and FDOM indices) in the surface water of the Mackenzie Delta Region during 4 expeditions from spring to fall in 2019, PANGAEA [dataset], 10.1594/PANGAEA.937582, 2021b.

Mulligan, R. P. and Perrie, W.: Circulation and structure of the Mackenzie River plume in the coastal Arctic Ocean, Continental Shelf Research, 177, 59-68, 10.1016/j.csr.2019.03.006, 2019.

Neweshy, W., Planas, D., Tellier, E., Demers, M., Marsac, R., and Couture, R. M.: Response of sediment phosphorus partitioning to lanthanum-modified clay amendment and porewater chemistry in a small eutrophic lake, Environ Sci Process Impacts, 24, 1494-1507, 10.1039/d1em00544h, 2022.

Nghiem, S. V., Hall, D. K., Rigor, I. G., Li, P., and Neumann, G.: Effects of Mackenzie River discharge and bathymetry on sea ice in the Beaufort Sea, Geophysical Research Letters, 41, 873-879, 10.1002/2013GL058956, 2014.

Norton, S. A. and Shanley, J. B.: Rare earth element and phosphorus mobility depend on adsorption to Al-, Fe-, and Mn-oxyhydroxides in a headwater stream in Vermont, USA, Biogeochemistry, 168, 53, 10.1007/s10533-025-01241-8, 2025.

Opsahl, S., Benner, R., and Amon, R. M. W.: Major flux of terrigenous dissolved organic matter through the Arctic Ocean, Limnology and Oceanography, 44, 2017-2023, 10.4319/lo.1999.44.8.2017, 1999.

Pokrovsky, O. S., Manasypov, R. M., Loiko, S. V., Krickov, I. A., Kopysov, S. G., Kolesnichenko, L. G., Vorobyev, S. N., and Kirpotin, S. N.: Trace element transport in western Siberian rivers across a permafrost gradient, Biogeosciences, 13, 1877-1900, 10.5194/bg-13-1877-2016, 2016.

Pourret, O., Davranche, M., Gruau, G., and Dia, A.: Competition between humic acid and carbonates for rare earth elements complexation, J Colloid Interface Sci, 305, 25-31, 10.1016/j.jcis.2006.09.020, 2007a.

Pourret, O., Davranche, M., Gruau, G., and Dia, A.: Organic complexation of rare earth elements in natural waters: Evaluating model calculations from ultrafiltration data, Geochimica Et Cosmochimica Acta, 71, 2718-2735, 10.1016/j.gca.2007.04.001, 2007b.

Pourret, O., Davranche, M., Gruau, G., and Dia, A.: Rare earth elements complexation with humic acid, Chemical Geology, 243, 128-141, 10.1016/j.chemgeo.2007.05.018, 2007c.

R. Core Team: R: A Language and Environment for Statistical Computing (4.4.3), R Foundation for Statistical Computing, 2025.

Reimann, C. and Filzmoser, P.: Normal and lognormal data distribution in geochemistry: death of a myth. Consequences for the statistical treatment of geochemical and environmental data, Environ. Geol., 39, 1001-1014, 10.1007/s002549900081, 2000.

Retamal, L., Bonilla, S., and Vincent, W. F.: Optical gradients and phytoplankton production in the Mackenzie River and the coastal Beaufort Sea, Polar Biology, 31, 363-379, 10.1007/s00300-007-0365-0, 2008.

Revel, M., van Drimmelen, C. K. E., Weltje, L., Hursthouse, A., and Heise, S.: Effects of rare earth elements in the aquatic environment: Implications for ecotoxicological testing, Critical Reviews in Environmental Science and Technology, 55, 334-375, 10.1080/10643389.2024.2406992, 2025.

Rollinson, H. and Pease, V.: Using Geochemical Data, 2, Cambridge University Press, Cambridge, 10.1017/9781108777834, 2021.

Rood, S. B., Kaluthota, S., Philipsen, L. J., Rood, N. J., and Zanewich, K. P.: Increasing discharge from the Mackenzie River system to the Arctic Ocean, Hydrological Processes, 31, 150-160, 10.1002/hyp.10986, 2017.

https://doi.org/10.5194/egusphere-2026-266
Preprint. Discussion started: 23 January 2026

Schädel, C., Bader, M. K. F., Schuur, E. A. G., Biasi, C., Bracho, R., Čapek, P., De Baets, S., Diáková, K., Ernakovich, J., Estop-Aragones, C., Graham, D. E., Hartley, I. P., Iversen, C. M., Kane, E., Knoblauch, C., Lupascu, M., Martikainen, P. J., Natali, S. M., Norby, R. J., O'Donnell, Jonathan A., Chowdhury, T. R., Šantrůčková, H., Shaver, G., Sloan, Victoria L., Treat, C. C., Turetsky, M. R., Waldrop, M. P., and Wickland, K. P.: Potential carbon emissions dominated by carbon dioxide from thawed permafrost soils, Nature Climate Change, 6, 950-953, 10.1038/nclimate3054, 2016.

Seeberg-Elverfeldt, J., Schlüter, M., Feseker, T., and Kölling, M.: Rhizon sampling of porewaters near the sediment-water interface of aquatic systems, Limnol Oceanogr-Meth, 3, 361-371, 10.4319/lom.2005.3.361, 2005.

Semkin, P., Tishchenko, P., Pavlova, G., Barabanshchikov, Y., Tishchenko, P., Shvetsova, M., Shkirnikova, E., and Fedorets, Y.: O2 and CO2 Responses of the Synaptic Period to Under-Ice Phytoplankton Bloom in the Eutrophic Razdolnaya River Estuary of Amur Bay, the Sea of Japan, 10.3390/jmse10121798, 2022.

Škerlep, M., Laudon, H., Lidman, F., Engström, E., Rodushkin, I., and Sponseller, R. A.: Patterns and controls of rare earth element (REE) dynamics across a boreal stream network, Water Res., 276, 123237, 10.1016/j.watres.2025.123237, 2025.

Stein, R., Macdonald, R. W., Naidu, A. S., Yunker, M. B., Gobeil, C., Cooper, L. W., Grebmeier, J. M., Whitledge, T. E., Hameedi, M. J., Petrova, V. I., Batova, G. I., Zinchenko, A. G., Kursheva, A. V., Narkevskiy, E. V., Fahl, K., Vetrov, A., Romankevich, E. A., Birgel, D., Schubert, C., Harvey, H. R., and Weiel, D.: Organic Carbon in Arctic Ocean Sediments: Sources, Variability, Burial, and Paleoenvironmental Significance, in: The Organic Carbon Cycle in the Arctic Ocean, edited by: Stein, R., and MacDonald, R. W., Springer Berlin Heidelberg, Berlin, Heidelberg, 169-314, 10.1007/978-3-642-18912-8_7, 2004.

Tadayon, Y., Dutruch, L., Vantelon, D., Gigault, J., Dia, A., Pattier, M., and Davranche, M.: Are nano-colloids controlling rare earth elements mobility or is it the opposite? Insight from A4F-UV-QQQ-ICP-MS, Chemosphere, 364, 143164, 10.1016/j.chemosphere.2024.143164, 2024.

Takahashi, Y., Minai, Y., Ambe, S., Makide, Y., Ambe, F., and Tominaga, T.: Simultaneous determination of stability constants of humate complexes with various metal ions using multitracer technique, Sci. Total Environ., 198, 61-71, 10.1016/S0048-9697(97)05442-9, 1997.

Takahashi, Y., Hayasaka, Y., Morita, K., Kashiwabara, T., Nakada, R., Marcus, M. A., Kato, K., Tanaka, K., and Shimizu, H.: Transfer of rare earth elements (REE) from manganese oxides to phosphates during early diagenesis in pelagic sediments inferred from REE patterns, X-ray absorption spectroscopy, and chemical leaching method, Geochemical Journal, 49, 653-674, 10.2343/geochemj.2.0393, 2015.

Tang, J. W. and Johannesson, K. H.: Speciation of rare earth elements in natural terrestrial waters: Assessing the role of dissolved organic matter from the modeling approach, Geochimica Et Cosmochimica Acta, 67, 2321-2339, 10.1016/S0016-7037(02)01413-8, 2003.

Tang, J. W. and Johannesson, K. H.: Ligand extraction of rare earth elements from aquifer sediments: Implications for rare earth element complexation with organic matter in natural waters, Geochimica Et Cosmochimica Acta, 74, 6690-6705, 10.1016/j.gca.2010.08.028, 2010.

Tostevin, R., Shields, G. A., Tarbuck, G. M., He, T. C., Clarkson, M. O., and Wood, R. A.: Effective use of cerium anomalies as a redox proxy in carbonate-dominated marine settings, Chemical Geology, 438, 146-162, 10.1016/j.chemgeo.2016.06.027, 2016.

https://doi.org/10.5194/egusphere-2026-266
Preprint. Discussion started: 23 January 2026

Toyoda, K., Nakamura, Y., and Masuda, A.: Rare earth elements of Pacific pelagic sediments, Geochimica et Cosmochimica Acta, 54, 1093-1103, 10.1016/0016-7037(90)90441-M, 1990.

Vonk, J. E., Giosan, L., Blusztajn, J., Montlucon, D., Pannatier, E. G., McIntyre, C., Wacker, L., Macdonald, R. W., Yunker, M. B., and Eglinton, T. I.: Spatial variations in geochemical characteristics of the modern Mackenzie Delta sedimentary system, Geochimica Et Cosmochimica Acta, 171, 100-120, 10.1016/j.gca.2015.08.005, 2015.

Wall, F.: Rare Earth Elements, in: Encyclopedia of Geology, edited by: Elias, S., and Alderton, D., 680-693, 10.1016/B978-0-08-102908-4.00101-610.1016/b978-0-08-102908-4.00101-6, 2021.

Wen, Y. H., Liu, P., Wang, Q., Zhao, S. M., and Tang, Y. Z.: Organic Ligand-Mediated Dissolution and Fractionation of Rare-Earth Elements (REEs) from Carbonate and Phosphate Minerals, Acs Earth and Space Chemistry, 8, 1048-1061, 10.1021/acsearthspacechem.4c00009, 2024.

Ye, L. M., März, C., Polyak, L., Yu, X. G., and Zhang, W. Y.: Dynamics of Manganese and Cerium Enrichments in Arctic Ocean Sediments: A Case Study From the Alpha Ridge, Frontiers in Earth Science, 6, 10.3389/feart.2018.00236, 2019.

Young, F. L., Colman, B. P., Carter, A. M., de Lima, R. F., Shangguan, Q. P., Payn, R. A., and Degrandpre, M. D.: Variability and Controls of CO and Air-Water CO Fluxes in a Temperate River, J Geophys Res-Biogeo, 130, e2024JG008434, 10.1029/2024JG008434, 2025.

Zilber, L., Parlanti, E., and Fortin, C.: Impact of organic matter of different origins on lanthanum speciation, bioavailability and toxicity toward a green alga, Frontiers in Environmental Chemistry, 5, 10.3389/fenvc.2024.1342500, 2024.